Tribology Online

Japanese Society of Tribologists
http://www.tribology.jp/trol/

Vol. 14, No. 5 (2019) 353-358.
ISSN 1881-2198
DOI 10.2474/trol.14.353

Article

Tribological Behavior of Hydrophilic and Hydrophobic Surfaces in Atmosphere with Different Relative Humidity

Kanao Fukuda*, Sie Leeh Sheng and Zaid Ali Subhi

[1)] Malaysia-Japan International Institute of Technology (MJIIT), Universiti Teknologi Malaysia, Jalan Sultan Yahya Petra, 54100 Kuala Lumpur, Malaysia

*Corresponding author: Kanao Fukuda (fukuda.kl@utm.my)

Manuscript received 30 June 2019; accepted 09 September 2019; published 15 December 2019
Presented at the International Tribology Conference Sendai 2019, 17-21 September, 2019

Abstract

The significant influences of atmospheric humidity on tribological phenomena are widely recognized. Although the influencing mechanisms of the humidity have been studied for a long time, many of the previous explanations remain in the qualitative estimation of mechanisms particularly from chemical effects viewpoint. In order to elucidate how the adsorbed water on a surface influences tribological phenomena, the current authors conducted ball to ball scratch tests for austenitic stainless steel (JIS SUS304) and proposed the mechanisms from a physical/mechanical viewpoint. A singular phenomenon was found; a lateral force, which can be regarded as a friction resistance, at a downhill motion showed significantly higher value than that at an uphill motion. The phenomenon was hypothesized to be influenced by Laplace pressure effect at a meniscus formed due to adsorbed water on the surface. In this study, polytetrafluoroethylene (PTFE) as the hydrophobic material was tested in comparison with SUS304 to show that the adsorbed water layer causes the singular phenomenon. PTFE successfully prevented the singular phenomenon while SUS304 reproduced it. The equilibrium analysis of the ball showed that adsorbed water contributed to the increase of the coefficient of kinetic friction but not of negative normal force at the contact point of SUS304.

Keywords

adhesion, water adsorption, polytetrafluoroethylene, austenitic stainless steel, hydrophobic surface, hydrophilic surface

1 Introduction

It is widely recognized that the humidity in environmental gases gives substantial influences on sliding phenomena, especially under unlubricated conditions. Therefore, many pieces of research have been carried out to reveal the mechanisms of the humidity to influence the sliding phenomena with practical sizes, i.e. at least with millimeter-size [1-5]. The researches have shown that there are various influences of the humidity depending on the kinds of materials. The mechanisms of the various influences of the humidity tend to be explained qualitatively from the viewpoint of chemical reactions such as oxidation, corrosion, passivation, etc. This means that quantitative approaches from the physical or mechanical viewpoint are not performed sufficiently for the issues. Contrary, researches on atomic to nano-level contact issues such as atomic force microscope (AFM) have succeeded to some extent on quantitative explanations on the influences of adsorbed water on the surfaces of materials in contact [6-9]. The researches discuss the effects of the meniscus, which takes place at the micron-size contact area due to adsorbed water on the surfaces. In those researches, the sizes of the phenomena are much smaller than mechanical parts, which are used commonly, and materials as research objects are limited and different from those used for the mechanical parts.

Based on the above-mentioned understanding, the research group of the current authors has aimed to study quantitatively the issues of water adsorption and the influences of the adsorbed water on the contact and adhesion of a practical material i.e. austenitic stainless steel and the study clarified the followings. The amount of adsorbed water on the surface of austenitic stainless steel increases with the increase of the relative humidity (RH) of environmental atmosphere and reaches equivalent value to a water layer on the apparent surface area of the sample with a thickness of 60 nm [10]. The amount of adsorbed water increases with the increase in the surface roughness of the sample [11]. In the very early stage of the sliding of self-mated austenitic stainless steel shows an initial steady period (ISP) which does not show micron-level or larger adhesion phenomena and the length of ISP is shorter at medium RH than those at low or high RH [12, 13]. A ball-to-ball scratching test of austenitic stainless steel shows a singular

phenomenon that the lateral force observed at a downhill motion shows extraordinarily high value compared with that at an uphill motion especially in the atmospheric air with medium RH [14]. The detection of the singular phenomenon at medium RH corresponds with the findings of both the shortest ISP [13, 14] and the highest wear rate [1, 2] at medium RH in previous studies on metallic materials. The correspondence suggests that the further understanding of the singular phenomenon may play an important role to reveal the dominant mechanisms of RH to influence sliding phenomena.

In the previous study [14], it was hypothesized that the singular phenomenon might be caused by the enhanced adhesion force due to Laplace pressure exerted at meniscus, which formed at the contact area due to adsorbed water on the surface of balls. The current study aims to confirm if the adsorbed water causes the singular phenomenon and discuss the possible causes of the phenomenon including Laplace pressure. The research was done by comparing austenitic stainless steel (JIS SUS304) and polytetrafluoroethylene (PTFE) using the ball-to-ball scratching test. PTFE is widely recognized as a hydrophobic material, which has water contact angle larger than 110° while that of SUS304 ranges between 50° to 80°, and expected to avoid water adsorption on the surface [9].

2 Experimental methods

2.1 A ball-to-ball scratching tester

Figure 1 shows the physical model of a ball-to-ball scratching tester used for experiments [14]. Upper ball O and lower ball O', which have the same diameter R, scratched horizontally against each other with an overlapping distance of δ. O was set at the end of a lever arm, which was equipped with displacement target concentrically set with O, force sensors for lateral force $L(x)$ and actual load $W(x)$, dead load W_0, a fulcrum and a counter balance weight. The force sensors with Roberval mechanism on the arm have inevitable elastic deformation, which is considerably larger than that of other parts of the tester, when the forces are applied to the balls. The deformability of the sensors is described as spring rates of k_1 and k_2 in the figure. The fulcrum supports the lever as possible to swing vertically but not horizontally. The adjustment of the position of the counter balance weight allows the lever leveled horizontally when W_0 was not loaded. The displacement x of O' was realized by an open-loop servo-controlled linear actuator and a command value for the actuator was regarded as the increment in the displacement x, and the origin point of x-axis ($x = 0$) was set concentrically at the position of O when the lever was set horizontally.

Before a scratching test, load of W_0 was applied on the lever and an upper ball lever supporter supported the lever to be leveled horizontally. While the test, O' approached O with moving speed of v along x-axis, contacted O, scratched and moved O up/down, and then departed from O. The displacement $d(x)$ of the upper ball O was evaluated as the function of the travel distance x of the lower ball using a laser displacement sensor with an accuracy of 2 μm. $L(x)$ exerted on O was evaluated as the function of x using a load force sensor. The tester is an imposed displacement system and actual load $W(x)$ exerts between the balls when O' travels along x-axis and pushes up O. Since the sensor of the lever has inevitable vertical elastic deformation as described as a spring with k_2 shown in Fig. 1, the detachment of the lever from the supporter has a temporal delay from the time of the contact of O and O' that results in a gradual increase of $W(x)$ as shown in Fig. 2. After the detachment of the lever form the supporter, $W(x)$ maintained the constant value, which was resulted by W_0, until the lever contacted the supporter again, and then $W(x)$ decreased gradually until the elastic deformation was completely released. A force sensor was set on the lever to observe the change of $W(x)$ as the function of x. A part of ball-to-ball scratching test

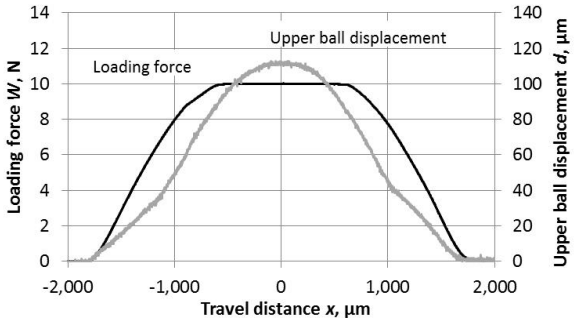

Fig. 2 Experimentally achieved loading force and the displacement of an upper ball

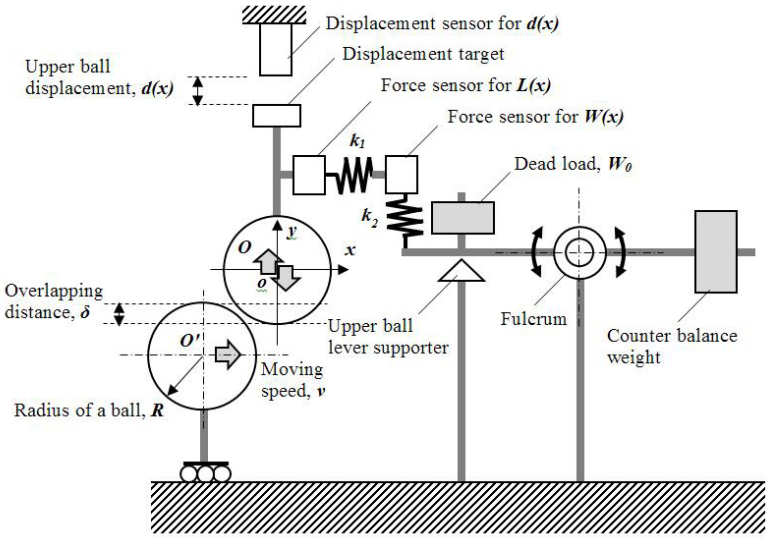

Fig. 1 Physical model of a ball-to-ball scratching test apparatus

was covered by a small semi-airtight chamber in which RH% controlled air was supplied prior to the scratching test. $d(x)$, $L(x)$ and $W(x)$ were synchronously measured and then recorded with x using A/D converter and computer [15, 16].

2.2 Variables in the experiments

The fixed independent variables in the experiments were dead load W_0, which was selected to make $W(x=0)$ to be 10 N., the moving speed v of O' at 2 mm·s^{-1}, $d(x=0)$, which is the expected maximum displacement of O, to be 110 μm by adjusting the height of O', and the radius of the ball samples R of 4 mm. The manipulated independent variables were the material of balls (SUS304 or PTFE) and RH% of atmospheric air (4, 55 or 95%). The monitored dependent variables in the tests were lateral force $L(x)$, loading force $W(x)$ and the displacement of the upper ball $d(x)$ as the functions of x.

2.3 Test procedure

The self-mated scratching tests were conducted for balls made of SUS304 or PTFE. In the case of SUS304, the surface of the balls was polished using a 0.3 μm diamond slurry to remove contaminations and an oxide layer, which inevitably exist on the surface of the samples with unknown antecedent. The balls are then ultrasonically cleaned in the mixture of acetone and hexane at 50:50 for 10 min., and dried before usage. It was confirmed that the surface roughness of the SUS304 balls was less than *Ra* 0.04 μm prior to the tests. In the case of PTFE, balls were used without polishing but with cleaning and drying since PTFE has low surface energy and no chemical compositions and stubborn contaminations are expected on the surface. After balls were set to the tester, air with controlled RH% was supplied at a flow rate of 2.5 L·min^{-1} for 60 min. to allow the amount of adsorbed water on the sample surfaces to saturated [11] before the scratching tests. The test for each material and each RH% condition was repeated 3 times with newly prepared specimens to confirm the repeatability of the test.

2.4 Contact conditions

Contact conditions of both materials at x=0 and $W(x=_0)$ of 10 N are estimated using Hertzian contact theory with Young's modulus and Poisson's ratio of 193 GPa and 0.3 for SUS304 and 0.62 GPa and 0.35 for PTFE, which were estimated values by the authors based on data from multiple sources. Maximum contact pressure, the radius of contact area and the depth of indentation are 1.76 GPa, 52 μm and 1.3 μm for SUS304 and 0.039 GPa, 350 μm and 61 μm for PTFE, respectively. Consequently, the estimated values of the initial overlapping distance δ are deduced by adding twice of the depth of indentation to 110 μm resulting in 113 μm and 232 μm for PTFE and SUS304, respectively. The estimated value of the maximum contact pressure in the case of SUS304 is less than the hardness of the material and an elastic deformation is supposed to take place. In case of PTFE, the maximum contact pressure is as low as 0.039 GPa and no plastic flow was observed on the surfaces of tested samples after scratching tests. Because of the differences in the material properties of SUS304 and PTFE, the contact conditions of these two materials are not able to adjust to be identical and $W(x=_0)$ of 10 N was commonly applied for both materials.

3 Results and discussion

Figure 2 shows the experimental results of $W(x)$ and $d(x)$ in the case of PTFE samples in the air with RH 95%. The results shown in Fig. 2 are considered as the ideal changes of $W(x)$ and $d(x)$ with the increase of x, which are close to the geometrically anticipated ones for the physical model shown in Fig. 1 without considerations on surface damages. The surfaces of PTFE balls after the test showed no significant damages while those of SUS304 balls had obvious marks of scratches. Due to the elastic deformation of the force sensors, $W(x)$ increased gradually up to 10 N with increase in x until the lever detached from the upper ball supporter, retained 10 N in the range of x between -660 and 660 μm and then, decreased gradually to 0 N after the lever contacted again with the supporter. The maximum value of $d(x)$ was 110 μm at x of 0 μm as set in the preparation of the test.

Figures 3 and 4 show experimentally obtained $L(x)$ and $W(x)$ for (a) SUS304 and (b) PTFE specimens in air with RH 4, 55 and 95%, respectively. 3 times tests of SUS304 at RH 95% and PTFE at all RH% showed good repeatability for both $L(x)$ and $W(x)$ while those for SUS304 in RH 4 and 55% showed large variety of data. For SUS304 tests in RH 4 and 55%, medium value results were shown in Figs. 3 and 4. In Fig. 3, the singular phenomenon, which was found in the previous research [14], was successfully reproduced in the case of SUS304 while the phenomenon was not observed in the case of PTFE regardless of the values of RH%. By observation on tested surfaces of SUS304 using an optical microscope, the significant scratch marks with the width of around 100 μm, which corresponded with estimated Hertzian contact radius of 52 μm, were found regardless of RH% values. The singular phenomenon observed for SUS304 in the current research is slightly different from that of the previous research [14]; the singular phenomenon shows the highest lateral force in the case of RH 95% in the current research while the phenomenon was not observed for RH 95% in the previous research. The difference might be caused by the

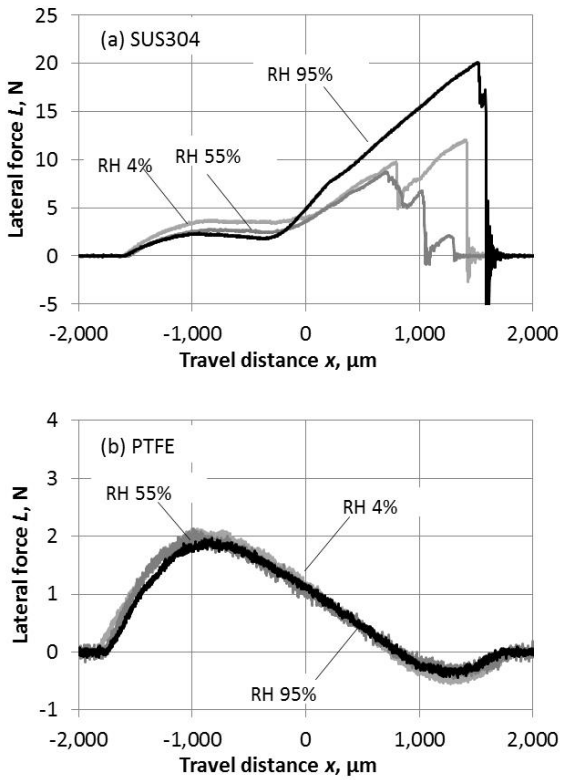

Fig. 3 Experimentally obtained lateral force as the functions of travel distance at different RH% for the self-mated scratching of (a) SUS304 and (b) PTFE

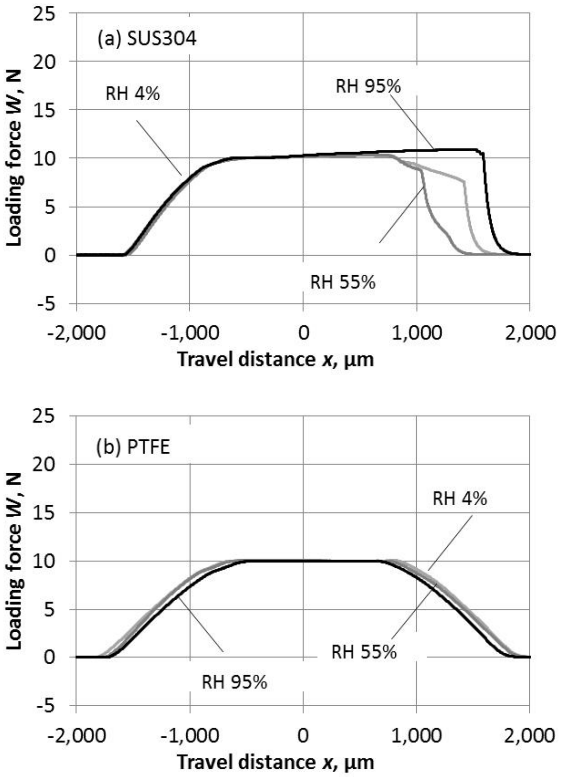

Fig. 4 Experimentally obtained loading force as the functions of travel distance at different RH% for the self-mated scratching of (a) SUS304 and (b) PTFE

difference in materials; JIS SUS316 was used in the previous research and the difference of surface finishing; ball specimens were used as purchased in the previous research. In the case of PTFE as shown in Fig. 3 (b), $L(x)$ was maintained as low as less than 2 N throughout the tests and particularly showed negative values in the downhill area regardless of the values of RH%.

In Fig. 4, $W(x)$ for (a) SUS304 shows unexpected high values comparing with the ideal changes shown in Fig. 2 in the rage of x larger than 0 μm while that for (b) PTFE shows quite similar changes to the ideal changes. The unexpected high values for SUS304 are supposed to be due to the elastic deformation of the force sensor for $L(x)$ shown in Fig. 1. Due to the large $L(x)$ in the rage of x larger than 0 μm shown in Fig. 3 (a), the sensor might deform towards positive direction along x-axis and the deformation allowed $W(x)$ to maintain high value by bearing W_0 even after x became larger than 1,000 μm.

For a further study on the phenomena observed in Figs. 3 and 4 including the negative value of $L(x)$, which appeared in Fig. 3 (b), the free-body diagram of ball-to-ball contact was considered as shown in Fig. 5. Here $N(x)$ and $F(x)$ are normal force and friction force exerted at the contact point on O, respectively. From the equilibrium of the forces exerted on O as shown in Fig. 6, $-L(x)$, which is detected by the load cell as the reaction force of the lateral force, was deduced theoretically as

$$N(x) = L(x)\cdot\cos(\alpha(x))+W(x)\cdot\sin(\alpha(x)) \quad (1)$$

$$F(x) = L(x)\cdot\sin(\alpha(x))-W(x)\cdot\cos(\alpha(x)) \quad (2)$$

$$\mu(x) = F(x)/N(x) \quad (3)$$

$$-L(x) = W(x)\cdot\{\cos(\alpha(x))+\mu\cdot\sin(\alpha(x))\}/\{\sin(\alpha(x))-\mu\cdot\cos(\alpha(x))\} \quad (4)$$

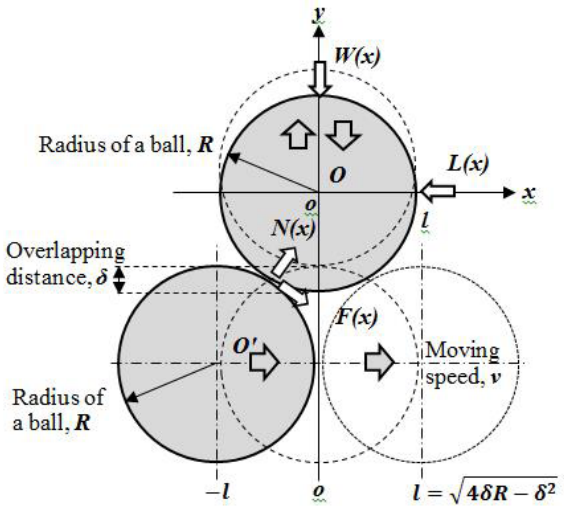

Fig. 5 Statics of ball-to-ball contact

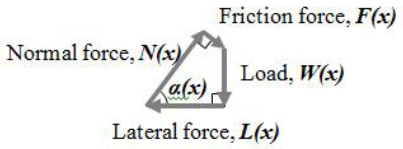

Fig. 6 An equilibrium of the forces exerted on an upper ball

Here $\mu(x)$ is the coefficient of kinetic friction at the point of the contact, $\alpha(x)$ is the angle between the direction of $N(x)$ and x-axis, which is derived geometrically from Fig. 5 as shown in Eq. (5).

$$\alpha(x) = -\cos^{-1}((-x)/(2\cdot R)) \quad (5)$$

The balls are geometrically in contact with each other in the range of x from $-l$ to l.

In the previous research [14], the difference between the phenomena happened in $x < 0$ and $x > 0$ regions in Fig. 5 was discussed to know why the singular phenomenon happened in the region of $x > 0$. A hypothesis proposed was that the adhesion force due to Laplace pressure at meniscus formed between the balls might cause the singular phenomenon because the force exerted when the contact area between the balls decreased in the region of $x > 0$. In this study, forces normal and parallel to the sliding surface, i.e. $N(x)$ and $F(x)$ are discussed in detail to know if. $N(x)$ shows significant tensile force in the particular region. Assuming $\mu(x)$ as constant values of 0, 0.05, 0.10, 0.15, 0.20, and 0.25, respectively, and using the experimental data of $W(x)$ obtained in Fig. 2, theoretical $L(x)$ was evaluated as shown in Fig. 7. The theoretical $L(x)$, which consists of only four forces shown in Fig. 6, successfully mimicked not only the negative value but also the whole shape of the changes of $L(x)$ appeared in experimental data Fig. 3 (b). By comparison between forms of the data appeared in Figs. 3 (b) and 7, the estimated value of μ in the experiments of PTFE is around 0.12 regardless of the values of RH%. 0.12 as the value of coefficient of kinetic friction is equivalent but slightly larger than the value reported in the previous research [17]. This result shows that the 4 forces shown in Fig. 6 and constant μ are major factors which govern the phenomena of sliding of PTFE regardless of the value of RH%. On the other hand, the shape of the changes of $L(x)$ in the case of SUS304 shown in Fig. 3 (a) is significantly different from those in Fig. 7. This means that the 4 forces in Fig. 6 and

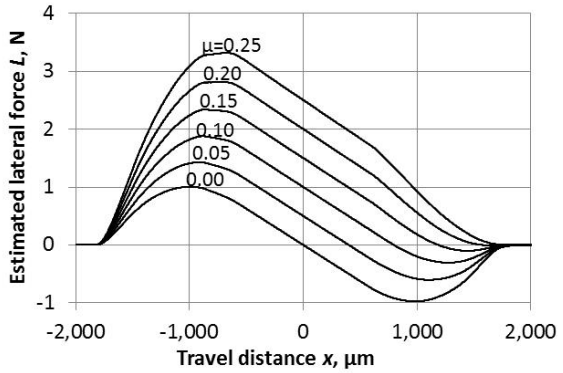

Fig. 7 Theoretical lateral force deduced using experimental load data

constant μ are not able to explain the singular phenomenon observed for SUS304.

To analyze the singular phenomenon of SUS304, $\mu(x)$ was deduced from experimental data $L(x)$ and $W(x)$ using Eqs. (1), (2) and (3), respectively. Both deduced $N(x)$ for (a) SUS304 and (b) PTFE in Fig. 8 showed similar behavior to those of $W(x)$ in Fig. 4, respectively. In case of (a) SUS304, the high values of $N(x)$ observed in the rage of x larger than 0 μm are supposed to be attributed to the elastic deformation of force sensor for $L(x)$ shown in Fig. 1 as same as the case of $W(x)$. Another notable behavior of $N(x)$ for SUS304 is a spike appears at the position where $N(x)$ value suddenly decreases, which infers a stick and slip motion due to adhesion. The position of spike is supposed to be identical to the position where the elastic deformation of the sensor is released. More importantly, $N(x)$ did not show negative values regardless of the x position. This suggests that the hypothesis in previous research [14] may not be the main mechanism of the singular phenomenon. Laplace pressure should originate significant adhesion, which is the negative direction for $N(x)$, and the tensile force due to adhesion should appear when the balls detached from each other if the force is large enough to cause such the large lateral force shown in Fig. 3 (a).

Figure 9 shows $F(x)$ for (a) SUS304 and (b) PTFE, respectively. It is obvious that large difference in $L(x)$ between SUS304 and PTFE is attributed to the difference in $F(x)$ between them. The coefficient of kinetic friction $\mu(x)$ for both sliding system were deduced using $N(x)$ and $F(x)$ as shown in Fig. 10. High value of $\mu(x)$ is observed at the point where the balls started contact with each other in the case of (a) SUS304. The sliding condition was identical for both balls because the movement of the balls is symmetrical about the point of contact; a way forward was untouched surface with saturated adsorbed water layer and a way backward was slid surface covered with residue of water after squeeze by the counterpart while the test except for the point of the first contact. The increase in $\mu(x)$ is also significant in the range x larger than 0, i.e. at the downhill motion area, for (a) SUS304 while $\mu(x)$ is almost constant for (b) PTFE. This singular phenomenon for SUS304 is clearly influenced by RH% and adsorbed water on the surface should cause this. In the case of PTFE, no significant differences by the level of RH% should be attributed to the absence of adsorbed water molecules on the PTFE due to hydrophobicity of its surface.

Although the experimental results obtained in this research could not provide enough evidences to judge if the hypothesis of the previous study [14] was accepted or rejected, high possibility was shown for the adsorbed water to influence

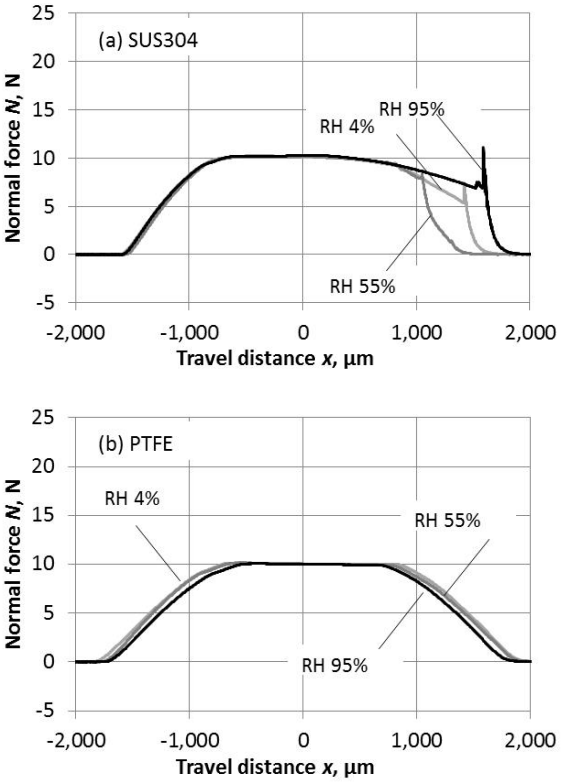

Fig. 8 Normal force at the contact point of the balls deduced from the experimentally obtained loading and lateral forces for (a) SUS304 and (b) PTFE

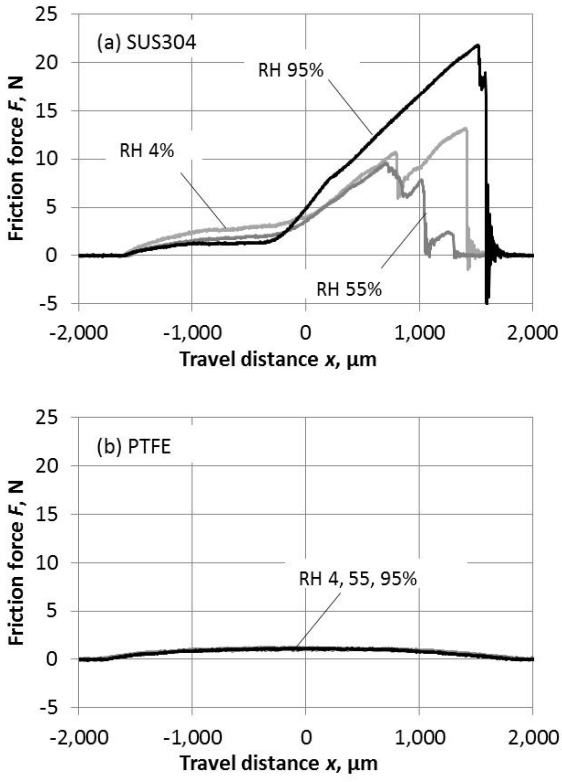

Fig. 9 Friction force at the contact point of the balls deduced from the experimentally obtained loading and lateral forces for (a) SUS304 and (b) PTFE

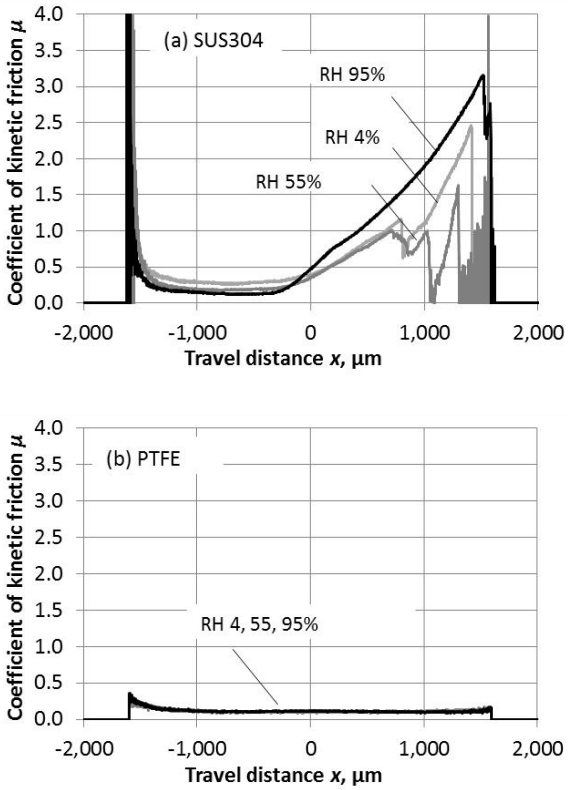

Fig. 10 Coefficient of kinetic friction at the contact point of the balls deduced from the experimentally obtained loading and lateral forces for (a) SUS304 and (b) PTFE

the singular phenomena by the comparison between SUS304 and PTFE. The possibility of another mechanism is suggested by detailed observation on the starting point of the singular phenomenon. It is obvious that $\mu(x)$ started to increase in the $x < 0$ and this is supposed to be due to severe adhesion, which takes place at metallic contact between balls. Since the amount of adsorbed water on the surface of SUS304 largely depends on RH% [10, 11], the difference in the amount of water may influence the degree of adhesion between the balls and its duration. It is interesting that thick water layer equivalent to 60 nm on the smooth surface enhanced adhesion as shown in this study while that on rougher surface prevented severe adhesion as shown in the previous study [14].

This research converted $W(x)$ and $L(x)$ into $N(x)$ and $F(x)$ to clarify that the singular phenomenon is identical to the increase in $F(x)$ and showed 2 direction of future research. One of them is to study $F(x)$ with the influencing factors at the interface. Another is to study the detailed component of $N(x)$ including the possibility of Laplace pressure. For the later one, it is necessary to obtain more detailed knowledge on the state of the adsorbed water on the materials such as the thin icelike layer consists of water molecules [18].

4 Conclusions

The self-mated ball-to-ball scratching test of PTFE did not show a singular phenomenon, which was the generation of extraordinarily high lateral force at the downhill motion, while the tests of SUS304 successfully reproduced the phenomenon. The phenomenon is supposed to be caused by the adsorbed water on the surface of SUS304 due to RH in atmosphere since the phenomena was not observed for the tests of PTFE, which is known to have no adsorbed water layer on the surface. Not enough evidences were obtained to proof that the singular phenomenon was caused by Laplace pressure at meniscus formed at the area of contact. Further study on influencing factors due to adsorbed water on friction force and normal force was suggested.

References

[1] Goto, H. and Buckley, D. H., "The Influence of Water Vapour in Air on the Friction Behaviour of Pure Metals during Fretting," Tribology International, 18, 4, 1985, 237-245.

[2] Fukuda, K., Norose, S. and Sasada, T., "Effect of Humidity on Sliding Wear in Fe and Cu Rubbing System," Proc. 28th Japan Congress on Materials Research, 1985, 89-92.

[3] Sasaki, S., "The Effects of the Surrounding Atmosphere on the Friction and Wear of Alumina, Zirconia, Silicon Carbide and Silicon Nitride," Wear, 134, 1, 1989, 185-200.

[4] Lancaster, J. K., "A Review of the Influence of Environmental Humidity and Water on Friction, Lubrication and Wear," Tribology International, 23, 6, 1990, 371-389.

[5] Barthel, A. J., Gregory, M. D. and Kim, S. H., "Humidity Effects on Friction and Wear between Dissimilar Metals," Tribology Letters, 48, 3, 2012, 305-313.

[6] Scherge, M., Li, X. and Schaefer, J. A., "The Effect of Water on Friction of MEMS," Tribology letters, 6, 3-4, 1999, 215-220.

[7] Ando, Y., "The Effect of Relative Humidity on Friction and Pull-Off Forces Measured on Submicron-Size Asperity Arrays," Wear, 238, 1, 2000, 12-19.

[8] Riedo, E., Levy, F. and Brune, H., "Kinetics of Capillary Condensation in Nanoscopic Sliding Friction," Physical Review Letters, 88, 18, 2002, 185505.

[9] Ohmae, N., "Humidity Effects on Tribology of Advanced Carbon Materials," Tribology International, 39, 12, 2006, 1497-1502.

[10] Subhi, Z. A., Fukuda, K., Morita, T. and Sugimura, J., "Quantitative Estimation of Adsorbed Water Layer on Austenitic Stainless Steel," Tribology Online, 10, 5, 2015, 314-319.

[11] Manaf, N. D. A., Fukuda, K., Subhi, Z. A. and Radzi, M. F. M., "Influences of Surface Roughness on the Water Adsorption on Austenitic Stainless Steel," Tribology International, 136, 2019, 75-81.

[12] Subhi, Z. A., Morita, T. and Fukuda, K., "Analysis of Humidity Effects on Early Stage of Sliding," Procedia Engineering, 68, 2013, 199-204.

[13] Subhi, Z. A., Fukuda, K., Morita, T. and Sugimura, J., "Analysis on the Mechanism of Humidity to Influence the Very Early Stage of Sliding under Different Load," Tribology Online, 10, 6, 2015, 420-427.

[14] Subhi, Z. A. and Fukuda, K., "Analysis on the Early Stage of Contact Adhesion in Different Relative Humidity," Malaysia-Japan Joint International Conference (MJJIC 2016), Seri Pacific Hotel, Kuala Lumpur, Malaysia, 6-7, 2016.

[15] Fukuda, K., "Friction Force Distribution and Its Alternation with Repeated Sliding System," Journal of Japanese Society of Tribologists, 43, 9, 1998, 788-795 (in Japanese).

[16] Fukuda, K., "Analysis of Specimen Displacement in Repeated Sliding System," Journal of Japanese Society of Tribologists, 49, 9, 2004, 738-745 (in Japanese).

[17] Biswas, S. K. and Vijayan, K., "Friction and Wear of PTFE – A Review," Wear, 158, 1-2, 1992, 193-211.

[18] Asay, D. B. and Kim, S. H., "Evolution of the Adsorbed Water Layer Structure on Silicon Oxide at Room Temperature," J. Phys. Chem. B., 109, 35, 2005, 16760-16763.